Fuel xxx (xxxx) xxx

Contents lists available at ScienceDirect

Fuel

journal homepage: www.elsevier.com/locate/fuel

Full Length Article

Raising the Research Octane Number using an optimized Simulated Moving Bed technology towards greater sustainability and economic return

Tasneem Muhammed [a], Begum Tokay [b], Alex Conradie [a,*]

[a] Sustainable Process Technologies Research Group, Faculty of Engineering, University of Nottingham, Nottingham NG7 2RD, UK
[b] Advanced Materials Research Group, Faculty of Engineering, University of Nottingham, Nottingham NG7 2RD, UK

ARTICLE INFO

Keywords:
Light naphtha isomerization process
Research Octane Number
Simulated Moving Bed
Adsorption
Genetic algorithm
Gross Margin optimization

ABSTRACT

The scale of CO_2 emissions from light-duty vehicle (LDV) fleets worldwide has led governments to mandate substantive improvements in vehicle fuel economy, thereby mitigating climate change. Raising the Research Octane Number (RON) of fuel through isomerization, alongside mandates to recalibrate existing LDV engines, promises to contribute substantially to climate action. This study has aimed to develop a highly efficient adsorption separation technology for isomerization refining that can contribute significantly to the sustainability and economics of the overall "well-to-wheel" outcome for LDV fleets globally. This study developed a rigorous dynamic model for a Simulated Moving Bed (SMB), comparing the SMB to conventional distillation as the next best alternative. The SMB was optimized using a genetic algorithm, maximizing RON and Gross Margin as objective functions. This study showed that SMB effectively separates high octane components from low octane components, producing a fuel with a RON of 95 when maximizing the RON, thereby enabling lower emissions associated with recalibrated LDV engines. Compared to 11 MW of steam duty associated with conventional distillation, the SMB unit utilized 3.4 MW and 5.7 MW of electricity when optimizing the RON and the Gross Margin respectively, appreciably reducing comparative greenhouse gas emissions. Finally, compared to conventional distillation as measured by Gross Margin, the optimized SMB unit increased the economic return by 47% when maximizing the RON and by 82 % when maximizing the Gross Margin. In summary, this study motivated for rapid capital investment into retrofitting isomerization facilities with SMB unit operations, replacing outmoded distillation as the primary separation technology. Future work will focus on optimizing the separation technology alongside the overall isomerization process using a rigorous techno-economic analysis as the objective function for optimization.

1. Introduction

The scale of CO_2 emissions from light-duty vehicle (LDV) fleets worldwide has led governments to mandate substantive improvements in vehicle fuel economy and appreciable reductions in CO_2 and other greenhouse gas (GHG) emissions from combustion engines, thereby mitigating climate change. As such, the efficiency of spark ignition engines is proportional to the engine compression ratio. New engine technologies with higher compression ratios require fuels with higher Research Octane Number (RON), where such fuels suppress auto-ignition before fuel consumption by the spark-initiated flame. However, assuming the availability of higher RON fuels, the roll-out of new engines with higher compression ratios has a time scale of decades [1]. Given the immediacy demanded by climate action, it is imperative to harness the substantial capital investment into existing LDV fleets to achieve climate action goals. Even modest efficiency improvements can provide substantial mitigation to the billions of tonnes of CO_2 emitted by LDV fleets annually. In this light, it is feasible to recalibrate existing engines which would allow for efficiency gains between 0.6 % (lightest load test cycle) and 4.4 % (heaviest load test cycle) [2]. Although a fuel's bio-ethanol content increases the RON, the energy density of ethanol limits its beneficial contribution to fuel blends. Therefore, raising the RON through isomerization of the linear alkane content in fossil reserves remains crucial to slow the pace of climate change. Refineries thus require cost-effective and resource-resilient solutions to raise the RON,

Abbreviations: BTCS, Backward Time Centred Space; FDM, Finite Difference Method; PDEs, Partial Differential Equations; PSA, Pressure Swing Adsorption; RON, Research Octane Number; SMB, Simulated Moving Bed.

* Corresponding author.
E-mail address: alex.conradie@nottingham.ac.uk (A. Conradie).

https://doi.org/10.1016/j.fuel.2022.126864
Received 11 September 2022; Received in revised form 18 November 2022; Accepted 20 November 2022

Nomenclature

List of symbols

b	Adsorption affinity constant (kPa^{-1})
b^0	Frequency factor of the affinity constant (kPa^{-1})
c_i	Concentration of component *i* in the fluid ($kmol \cdot m^{-3}$)
$C_{p,i}$	Purchase cost of equipment *i*
D_{ax}	Axial mass dispersion coefficient ($m^2 \cdot s^{-1}$)
D/F	Molar Desorbent / Feed Ratio (%)
E	Activation energy ($kJ \cdot mol^{-1}$)
F	Molar flow rate ($kmol \cdot h^{-1}$)
H	Operating hours per annum
I_{2021}	Cost index in year 2021
I_b	Cost index in year *b*
IT	Indexing Time (min)
k_f	Annualizing factor
k_{MTCi}	Effective mass transfer coefficient of component *i* (s^{-1})
M_w	Molecular weight ($g \cdot mol^{-1}$)
n	Facility life time (years)
P	Price or cost ($)
p_i	Partial pressure of sorbate i (kPa)
P	Pressure (kPa)
P_o	Operating pressure (kPa)
ΔP	Pressure drop (kPa)
$\bar{q}_i$	Average amount of solute *i* adsorbed ($kmol \cdot kg_{ads}^{-1}$)
q_i^*	Equilibrium loading of component *i* ($kmol \cdot kg_{ads}^{-1}$)
q_i	Amount adsorbed of component *i* ($mol \cdot m^{-3}$)
q_m	Saturation loading of component *i* ($mol \cdot m^{-3}$)
Q	Utility duty (MW)
r_p	Particle radius (m)
R	Gas constant (8.314 $J \cdot mol^{-1} \cdot K^{-1}$)
t	Time (s)
T	Temperature (K)
v_g	Gas velocity ($m \cdot s^{-1}$)
W	Work (MW)
x	Space (m)
x_i	Molar fraction of component *i* (%)

Greek symbols

ε_b	Interstitial voidage ($m^3_{void} \cdot m^{-3}_{bed}$)
ε_t	Total bed voidage ($m^3_{(void+bed)} \cdot m^{-3}_{bed}$)
ρ	Construction material density ($kg \cdot m^{-3}$)
ρ_b	Adsorbent bulk density ($kg \cdot m^{-3}$)
ρ_g	Gas phase density ($kg \cdot m^{-3}$)
η	Efficiency (%)
γ	Specific heat capacity ratio
μ_g	Dynamic viscosity ($N \cdot s \cdot m^{-2}$)

Subscripts

H	High
L	Low

Mathematical symbols

∂	Partial differential
d	Ordinary differential
Δ	Change (step size)
Σ	Summation
π	Ratio of a circle's circumference to its diameter
exp	Exponential function
f	Function
j	Time coordinate index
i	Axial coordinate index
t	Number of time elements
x	Number of space elements

where these solutions significantly improve the sustainability and economics of the overall "well-to-wheel" outcome, i.e. (1) Enable lower GHG emissions associated with existing LDV fleets, (2) Reduce the GHG emissions associated with refining and (3) Provide for greater economic return.

In fuel production via the isomerization of light naphtha, the single-pass process can produce fuel with a RON of 78–80 [3]. Integrating a separation process that recycles the linear alkanes typically recovers approximately 65 % of the fresh feed (i.e. light naphtha), improving the RON to 88–95 [4]. Conventionally, distillation columns are utilized to raise the RON [5–7]. However, distillation technology represents a significant capital burden, achieves a RON of only 80–92, and is energy intensive given the marginal boiling point difference between the linear and branched alkanes. Consequently, hybrid distillation/adsorption systems such as Hexorb™ (provided by AXENS) have been introduced commercially [8,9]. These systems improve the RON by 1–2 at a similar cost and energy consumption to conventional distillation. Although these technologies have delivered the targeted RON of 95 as mandated by governments [10], less energy-intensive and costly technologies are warranted.

From a sustainability viewpoint, there is a growing interest in alternative separation processes, meeting the RON requirement with reduced environmental impact and greater economic return. Adsorption separation technologies have proven advantages over distillation, raising the RON by 3–4. Various adsorbents such as zeolite 5A [11–14], zeolite BETA [15–17], ZIF-8 [18,19] and silica [20] have been widely investigated by researchers. Moreover, the performance of these adsorbents has been explored using mathematical models, fitting experimental data to model parameters. Previous modelling studies have compared adsorption performance investigating different zeolite structures [21], and have characterized the structural dynamics and adsorption properties of zeolites [22].

These zeolite adsorbents have been deployed in several Pressure Swing Adsorption (PSA) modes of operation; from batch, fixed bed adsorption [23–29] to more continuous cyclic adsorption systems [30–33]. From a process intensification perspective, the principal disadvantage of PSA processes is the sequential bed operation, where the bed is either subject to adsorption or desorption. Also, during sequential batch operation of a two-bed configuration, the equilibrium between the adsorbent and the feed is rapidly attained at the bed entrance, meaning this section of the bed is no longer adsorbing linear alkanes and is ineffectively awaiting desorption [34]. This section of the bed is thus purely a conduit for the feed to the lower sections of the bed that have not attained equilibrium with the feed. Compared to Simulated Moving Bed (SMB) technologies, the required adsorbent inventory for a two-bed configuration is three to four times larger, while in the case of desorption, twice the volume of desorbent is required [34]. Although SMB technologies are widely used in chemical processes such as sugar, pharmaceutical, and petrochemical applications, only one commercial option, UOP's Sorbex process, is available to raise the RON of fuels [34].

Therefore, this study aimed to develop a highly efficient adsorption separation technology that can address the abovementioned challenges, whilst significantly contributing to the sustainability and economics of the overall "well-to-wheel" outcome. The objectives of this study were, (1) Deliver a fuel with higher RON, enabling lower emissions associated with recalibrated LDV engines, (2) Reduce the GHG emissions associated with refining and (3) Provide for greater economic return. Turning to SMB technology as a solution, various operating parameters were considered as optimization decision variables, viz. Temperature (T), Adsorption Pressure (P), the Indexing Time (IT) and the Molar

Desorbent / Feed Ratio (D/F) expressed as a percentage of the feed rate. The optimization was realized using a genetic algorithm to explore the solution space presented by a rigorous SMB dynamic model, maximizing RON and Gross Margin as the objective functions. Finally, the SMB technology was compared to conventional distillation as a next best alternative technology.

2. Opportunity presented by Simulation Moving Bed technology

There are several SMB design and cycle strategies described in the literature [35,36]. An SMB unit is typically comprised of a number of packed beds arranged around a rotary, multi-port valve and includes auxiliary equipment such as hold-up tanks, control valves, and compressors. Fig. 1 illustrates the SMB process employed in this study which entails four operational zones [37]. The packed beds of the SMB unit remain fixed, while the feeds to each zone rotate stepwise through the beds of each zone via the rotary, multi-port valve. A reduced indexing (switching) time maximizes the utilization of the adsorbent inventory, lowering the required bed height; noting that from a number of cycles perspective, the adsorbent charge is preferably only replaced during the plant's annual shutdown. Consequently, the required fractionation efficiency determines the number of beds in each operational zone. In this study, an eight-bed SMB unit, i.e. two beds per zone, delivered the desired performance.

The SMB zones are described as follows with reference to Fig. 1. Each zone entails different feeds at different fluid flow rates relative to the effective counter-current solid (adsorbent) flow rate as governed by the Indexing Time. The feed mixture of linear and branched alkanes enters Zone I. Beds in this zone are operated at high pressure, selectively adsorbing the linear alkanes, allowing the branched alkanes to flow through the bed as Raffinate. The adsorbed linear alkanes are de-pressurized in Zone II and cycled from Zone II to Zone III. Zone III elutes the linear alkanes at low pressure, favouring desorption, using a suitable desorbent such as hydrogen. Zone IV pressurizes the beds prior to indexing into Zone I, noting that the adsorbent pores are saturated by the desorbent at the start of adsorption.

2.1. Rigorous mathematical model for SMB simulation

A rigorous partial differential equations model for the eight-bed SMB unit was coded in Matlab® 2020a. The governing equations of the model were derived based on the following assumptions:

1. Ideal gas behaviour.
2. Isothermal operation [16].
3. The dead volume on either side of a bed is negligible [38].
4. A linear driving force model describes the mass transfer between the fluid phase and the solid adsorbent phase [39].
5. A plug flow model with axial dispersion describes the dynamic system.
6. The Ergun equation defines the pressure drop [40].
7. The kinetic rate limiting step is the effective mass transfer, dictated by the film mass transfer and pore diffusion, of the components from the bulk fluid phase to the solid adsorbent surface [40].
8. The vapour-solid equilibrium is described by the Tri-Site Langmuir (TSL) isotherm [15].

The continuity equation in Eq. (1) governs the mass balance for each component [41].

$$\underbrace{\varepsilon_b D_{ax}\frac{\partial^2 c_i}{\partial x^2}}_{\text{Dispersion}} = \underbrace{\frac{\partial\left(v_g c_i\right)}{\partial x}}_{\text{Convection}} + \underbrace{\varepsilon_t\frac{\partial c_i}{\partial t}}_{\text{Accumulation}} + \underbrace{\rho_b\frac{\partial \bar{q}_i}{\partial t}}_{\text{Mass transfer}} \tag{1}$$

where ε_b is the interstitial voidage, c_i is the concentration of component i in the fluid, v_g is the gas velocity, ε_t is the total bed voidage, ρ_b is the adsorbent bulk density, x is the axial space coordinate along the length of the bed, t is the time coordinate, $\bar{q}_i$ is the average amount of i adsorbed and D_{ax} is the axial dispersion coefficient. The axial dispersion coefficient, D_{ax}, equals $1.155{\cdot}10^{-4}$ and $1.095{\cdot}10^{-4}$ $m^2{\cdot}s^{-1}$ for C5 and C6 alkanes (within 423–583 K) respectively [17].

The mass transfer term in Eq. (1) is described using the linear driving force model as per Eq. (2) [39,42].

$$\frac{\partial \bar{q}_i}{\partial t} = k_{MTCi}\cdot\left(\bar{q}_i - \mathrm{q}_i^*\right) \tag{2}$$

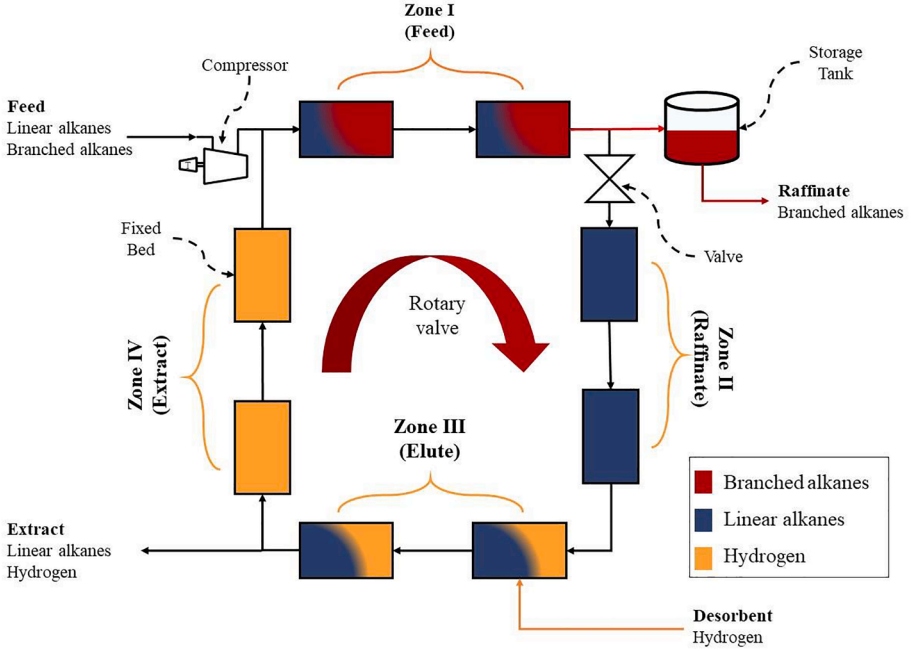

Fig. 1. Simulated Moving Bed (SMB) unit comprising four zones and eight packed beds. Each bed cycles through adsorption, de-pressurization, desorption and pressurization, allowing for the branched alkanes to be collected as Raffinate and the linear alkanes to be collected as Extract.

where k_{MTCi} is the effective mass transfer coefficient of component i and q_i^* is the equilibrium loading for component i.

The TSL isothermal model describes the equilibrium between the fluid and the solid adsorbent phase, given this equilibrium model structure effectively represents experimental data over a wide pressure range [15]. The isotherm is described by Eq. (3).

$$q_i = \sum_j \frac{q_{i,j}^m \cdot b_{i,j} \cdot p_i}{1 + \sum_i b_{i,j} \cdot p_i} \tag{3}$$

where q^m is the saturation loading in each site, p_i is the partial pressure for the component i, j is the number of sites and b_i is the adsorption affinity constant of component i in site j. The adsorption affinity constant (b_j) is described by the Arrhenius Eq. (4).

$$b_j = \mathrm{b}_j^0 \cdot e^{\left(\frac{-E_j}{R \cdot T}\right)} \tag{4}$$

where $b_j{}^0$ is the frequency factor of the affinity constant, E_j is the interaction energy of site j, T is the temperature and R is the universal gas constant.

As the momentum conservation equation, the Ergun equation describes the pressure drop as in Eq. (5), given the equation's validity over laminar as well as turbulent flow regimes [17].

$$-\frac{dP}{dx} = \frac{1.5 \cdot 10^{-3} \cdot \mu_g (1-\varepsilon_b)^2}{(2r_p)^2 \varepsilon_b^3} v_g + \frac{1.75 \cdot 10^{-5} \cdot M_w \rho_g (1-\varepsilon_b)}{(2r_p) \varepsilon_b^3} v_g^2 \tag{5}$$

where P is the pressure, μ_g is the dynamic viscosity and M_w is the average molecular weight.

The mass balance around the control volume of the Raffinate storage tank is modelled using Eq. (6) [43].

$$\frac{dF}{dt} = F_{in} - F_{out} \tag{6}$$

where F_{in} and F_{out} are the inlet and outlet flow rates respectively.

The work of the compressor model is described by Eq. (7) [44].

$$W = F \cdot R \cdot T \frac{1}{\eta} \frac{\gamma}{(1-\gamma)} \left[\left(\frac{P_H}{P_L} \right)^{\frac{\gamma-1}{\gamma}} - 1 \right] \tag{7}$$

where W is the work, F is the molar flow rate, η is the polytropic efficiency assumed to be 75 %, and γ is the specific heat capacity ratio, estimated as 1.334 using HYSYS® v10.

The SMB performance can be characterized for the high octane components, i.e. 2,3-dimethylbutane (23DMC4), 2,2 dimethylbutane (22DMC4), and isopentane (iC5), given these increase the RON; whereas the low octane components, i.e. *n*-pentane (nC5), 3-methylpentane (3MC5) and *n*-hexane (nC6) decrease the RON [16] (Table S1). The performance parameters were defined as Recovery, Purity, Productivity, and Desorbent Consumption [35]. The SMB performance parameters were calculated as follows [16,35].

$$Molar\ Recovery = \frac{F_{High\ octane\ components\ in\ Raffinate}}{F_{High\ octane\ components\ in\ feed}} \cdot 100 \tag{8}$$

$$Molar\ Purity = \frac{F_{High\ octane\ components\ in\ Raffinate}}{F_{Total\ components\ in\ Raffinate}} \cdot 100 \tag{9}$$

$$Specific\ Productivity = \frac{F_{High\ octane\ components\ in\ Raffinate}}{Mass\ of\ SMB\ adsorbent\ charge} \tag{10}$$

$$Desorbent\ Consumption = \frac{F_{Desorbent}}{F_{High\ octane\ components\ in\ Raffinate}} \tag{11}$$

2.2. Solution strategy

Each bed of the SMB unit is a dynamic system described by a non-linear set of partial differential equations (PDEs). This study employed a numerical integration solution, viz. the Backward Time Centred Space (BTCS) scheme to solve the set of PDEs. The BTCS scheme couples the finite difference method (FDM) and the explicit Euler's method [45]. The BTCS scheme approximates the integral using a finite element grid (mesh) in relation to space (x) and time (t). After attaining the maximum bed length and time in the calculation sequence, the state variables (i.e. c_i, P, and q_i) are defined at any point in the grid, providing an approximate solution to the set of PDEs.

Fig. 2 illustrates the numerical integration solution strategy to simulate the cycle of the SMB unit. The strategy is summarized as below:

1. The eight SMB beds are assumed to be one deep bed divided into 4 zones. Each zone includes two sections, and each section represents a bed.
2. At the entrance of the deep bed, the feed condition defines the initial condition and the initial adsorption loading of the solid phase is assumed to be zero.
3. Each section is discretized into space (x) and time (t) finite elements. Starting with the defined initial condition, the set of PDEs is solved using the BTCS scheme.
4. The solved PDEs provide a new initial condition, which is used to solve the next section.
5. The calculation strategy iterates to step 3 with the new initial condition and repeats until the total number of sections is solved.
6. Throughout this iterative process, desorbent is fed to Zone III and Raffinate and Extract are withdrawn from Zones I and Zone III respectively.
7. At the exit of the deep bed, the Extract is accumulated for recycle to the isomerization reactor. Thereafter, the bed adsorption loading at the maximum bed length is switched to the entrance of the deep bed to start a new cycle.
8. The cycle is repeated from step 2 until the maximum number of cycles is reached.
9. Finally, the cumulative outlet concentrations of both the Raffinate and the Extract are obtained.

In this study, the PDEs were discretized using 20 finite elements for time (t) and 10 finite elements for space (x).

3. Comparative economic analysis

The three objectives of this study necessitated optimization of the design and operating conditions of the SMB unit. The genetic algorithm implemented in Matlab® 2020a was utilized as optimization algorithm, maximizing the RON and Gross Margin as objective functions using the decision variables, viz. Temperature (T), Adsorption Pressure (P), Indexing Time (IT) and the Molar Desorbent / Feed Ratio (D/F) expressed as a percentage of the feed rate. The decision variables were bounded within the operating ranges summarized in Table 1.

As a comparative economic analysis, a conventional distillation process modelled in HYSYS® v10 was considered as the next best alternative in keeping with [7]. As one of the two objective functions, the Gross Margin was defined in Eq. (12).

$$Gross\ Margin = Revenue - Raw\ Material\ Cost - Utility\ Cost - Annualized\ Capital \tag{12}$$

where the terms Revenue, Raw Material Cost, Utilities Cost, and Annualised Capital are defined below.

The economic value of a fuel principally depends on its quantity and quality (i.e., RON). The following expression measures the revenue as per Eq. (13).

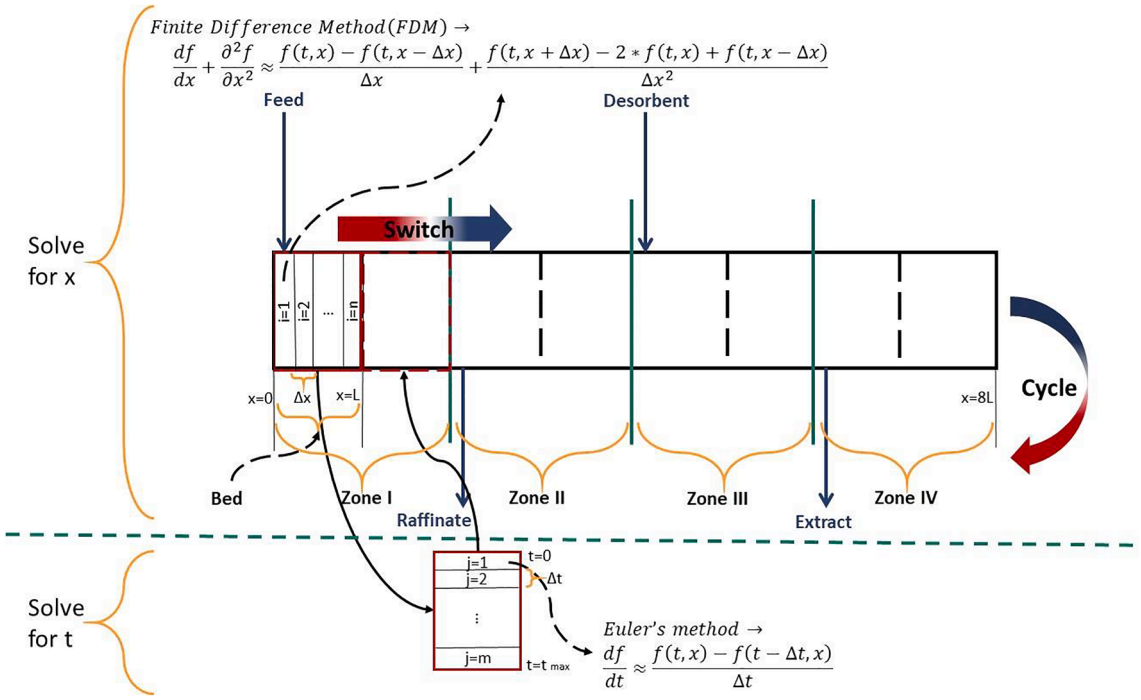

Fig. 2. Numerical integration solution strategy for the rigorous simulation of the Simulated Moving Bed (SMB) unit.

Table 1
Decision variables and bounds for the optimization of the Simulated Moving Bed operating conditions using a genetic algorithm.

Decision variables	Lower bound	Upper bound
Temperature (K)	423	583
Adsorption Pressure (bara)	11	19
Indexing Time (min)	1	15
Molar Desorbent / Feed Ratio (%)	1	100

$$Revenue = H \cdot \dot{V}_{Fuel} \cdot P_{Fuel} \tag{13}$$

where H is the operating hours per annum (8000 h), $\dot{V}_{Fuel}$ is the volumetric flow rate and the fuel price, P_{Fuel}, is described by Eq. (14), which was linearly formulated from data provided in Ref. [7].

$$P_{Fuel}\left(\$ \cdot m^{-3}\right) = 19.8 \cdot RON - 1061 \tag{14}$$

There are several models to estimate the RON [46,47]. In this study, a linear-by-mole approach was used to estimate the RON as shown in Eq. (15) [48].

$$RON = \sum_{i=1}^{n} RON_i \cdot x_i \tag{15}$$

where RON_i is the RON of pure component i (provided in Table S1), x_i is the molar fraction of component i, and n is the number of components.

The raw material and utility costs were calculated as per Eqs. (16) and (17).

$$Raw\ Material\ Cost = H \cdot \left(\dot{V}_{Light\ naphtha} \cdot P_{Light\ naphtha} + \dot{V}_{H_2} \cdot P_{H_2} \right) \tag{16}$$

$$Utility\ Cost = H \cdot \left(Q_{steam} \cdot P_{steam} + Q_{cooling\ water} \cdot P_{cooling\ water} + Q_{electricity} \cdot P_{electricity} \right) \tag{17}$$

where $\dot{V}$ is the volumetric flow rate at defined temperature and pressure, Q is the duty and P is the price or cost. The Raw Material and Utility Costs are summarized in Table S4. Note that the Raw Material Costs are identical for the comparison between the SMB unit and conventional distillation as separation technologies.

The annualised capital was estimated using Eq. (18).

$$Annualized\ Capital = k_f \cdot \sum_{i}^{n} C_{P,i} \tag{18}$$

where $C_{p,i}$ is the purchase cost of equipment i and k_f is the annualizing factor.

For each capital item, the purchase cost was adjusted given the time value of money to the year of the capital purchase, $C_{P,2021}$, using the Chemical Engineering Plant Cost Index (CEPCI) as per Eq. (19).

$$C_{P,2021} = C_{P,b} \cdot \frac{I_{2021}}{I_b} \tag{19}$$

where $C_{P,b}$ is the purchase cost (correlations are detailed in the Supplemental) in year b, I_b is the CEPCI cost index in year b, and I_{2021} is the CEPCI cost index in the year of the capital purchase (CEPCI = 708.0) [49]. For brevity, this comparative economic analysis omitted installation cost, the commissioning cost and the location factor from consideration.

The annualizing factor (k_f) was calculated using Eq. (20).

$$k_f = \frac{i \cdot (1+i)^n}{(1+i)^n - 1} \tag{20}$$

where i reflects the cost of capital ($i = 0.15$) and n is the facility life time in years (n = 20 years).

4. Results and discussion

This study evaluated a refining facility processing 10,000 barrels per day of light naphtha, equating to a reactor effluent flow rate of 500 kmol·h^{-1} as feed to either the SMB or the distillation (next best alternative) separations technology. As summarized for the base case in Table 2, the SMB was simulated isothermally, exploiting the adsorption selectivity through pressure swing [25,29]. The thermodynamic and kinetic parameters were determined previously from experimental data

Table 2
Base case Simulated Moving Bed sizing, bed properties and operating conditions.

Equipment dimensions	Base case
Number of beds	8
Diameter (m)	3.33
Length (m)	6.67
Bed properties	
Total bed voidage (ε_t)	0.49
Interstitial voidage (ε_b)	0.35
Adsorbent particle diameter (m)	$1.59{\cdot}10^{-3}$
Bulk density (ρ_b) (kg·m^{-3})	750
Operating conditions	
Temperature (K)	523
Low Pressure Swing (bara)	5
High Pressure Swing (bara)	15
Indexing Time (min)	7
Linear velocity (m·s^{-1})	
Feed	$0.36{\cdot}10^{-3}$
Raffinate	$0.94{\cdot}10^{-3}$
Desorbent	$1.53{\cdot}10^{-3}$
Extract	$2.11{\cdot}10^{-3}$

[17], where the mass transfer coefficients and extended Langmuir parameters are summarized in Tables S2 and S3 respectively.

Simulating the rigorous model using these base case model parameters, Fig. 3 shows the dynamic response of the component concentrations and RON (Fig. 3C) for the Raffinate (Fig. 3A) and Extract (Fig. 3B), achieving steady state from start-up after 20 cycles as is typical for hydrocarbon separations [38]. Given the nominal Indexing Time (Table 2), the SMB unit achieved steady state after approximately 2.5 h. Isopentane (iC5) was predominantly fractionated and concentrated into the Raffinate attaining 0.38 kmol·m^{-3}, while linear pentane (nC5) was fractionated and concentrated into the Extract attaining 0.35 kmol·m^{-3}. The Raffinate attained a RON of 92.2, whereas the Extract attained a RON of 62.5 for recycle to the isomerization reactor. Table 3 summarizes the base case performance parameters and Fig. 4 details the base case material balance around the control volume of the SMB unit after achieving steady state.

Table 3
Simulated Moving Bed base case performance parameters.

Performance parameters	Base case
Raffinate RON	92.2
High octane	
Recovery (mol%)	85.4
Purity (mol%)	99.97
Specific Productivity (mol·(kg adsorbent)$^{-1}$·h^{-1})	0.67
Desorbent Consumption (mol/mol)	0.64

4.1. Comparative economic analysis

The three objectives of this study necessitated optimization of the aforementioned base case performance of the SMB unit. After maximizing the RON as objective function using the genetic algorithm, the RON for the SMB base case was increased from 92.2 to 95 (Table 4, Fig. 5B). Similarly, after maximizing the Gross Margin as the objective function using the genetic algorithm, the Research Octane Number (RON) for the SMB base case was increased from 92.2 to 93.1 (Table 4, Fig. 5B). Both the base and optimized SMB cases improved the RON compared to the RON of 90.9 achieved through conventional distillation (Table S6, Fig. 5B). Thereby, the optimized SMB cases (Figs. S1 and S2) delivered a fuel with higher RON, enabling lower emissions associated with recalibrated LDV engines. The genetic algorithm maximised the RON and the Gross Margin by decreasing the SMB operating Temperature to 427 K and 447 K respectively (Table 4). Maximizing the RON required a lower adsorption Pressure, while maximizing the Gross Margin required a higher adsorption Pressure and Indexing Time (Table 4). From the Purity (Table 4), the base and optimized SMB cases all demonstrated highly selective fractionation of the low octane components into the Extract. Given the feed composition, the inclusion of isopentane (iC5), a high octane component, in the Extract is necessary to attain a RON > 91 (iC5, Table S1) in the Raffinate. From the material balances (Fig. 4 and S1, S2); the higher the RON, the greater the

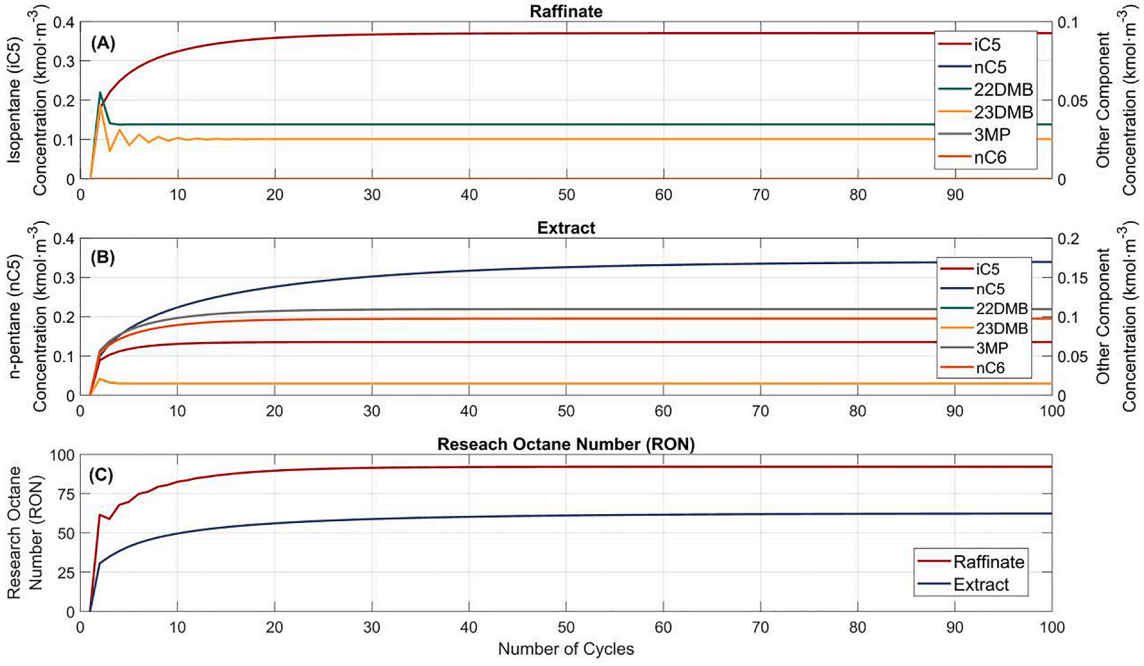

Fig. 3. Dynamic response of the component concentrations (A, B) and RON (C) for the Raffinate (A) and Extract (B), showing the approach to steady state from start-up over 100 cycles.

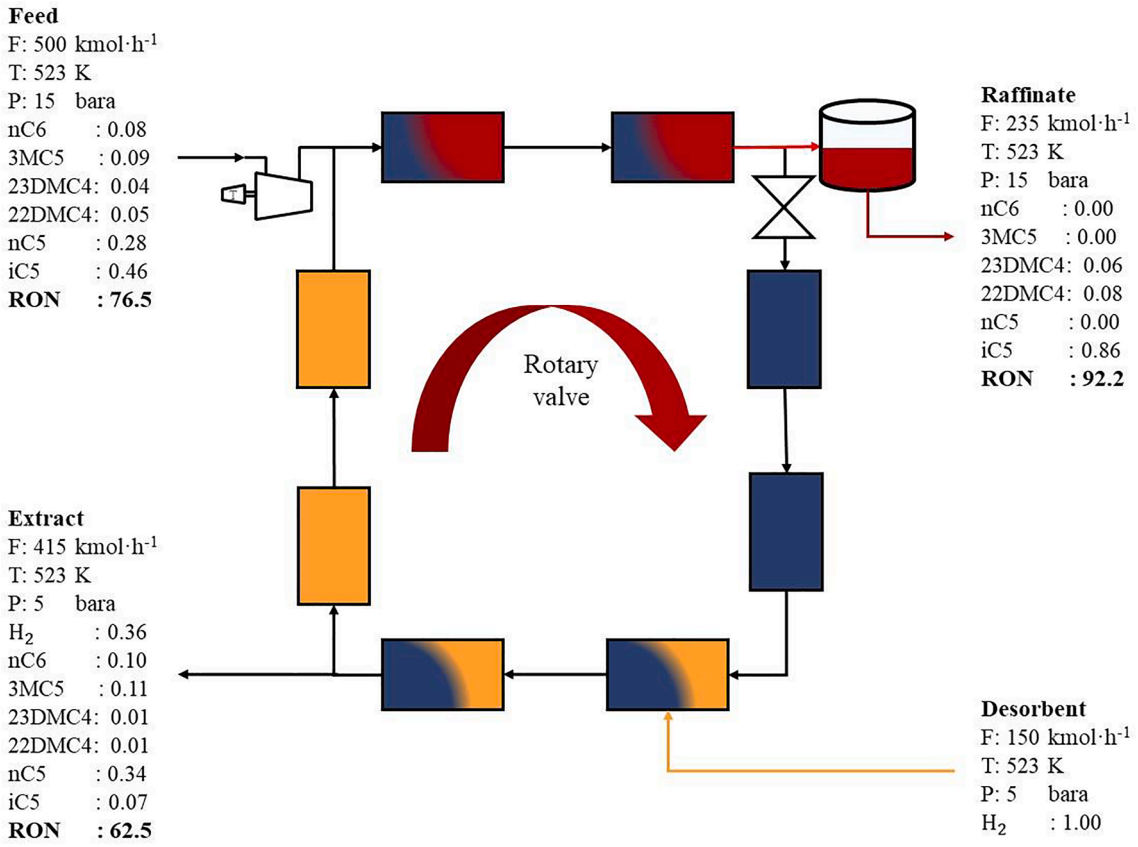

Fig. 4. Base case material balance around the control volume of the SMB unit after attaining steady state.

Table 4
Simulated Moving Bed base case and optimized performance parameters.

Performance parameters	Base case	RON optimized	Gross Margin optimized
Gross Margin ($ Millions·annum^{-1})	46.6	41.1	50.8
Raffinate RON	92.2	95	93.1
High octane			
Recovery (mol%)	85.4	34.5	70
Purity (mol%)	99.97	100	100
Specific Productivity (mol·(kg adsorbent)$^{-1}$·h^{-1})	0.67	0.27	0.55
Desorbent Consumption (mol/mol)	0.64	1.58	0.78
Electricity (MW)	5	3.4	5.7
Decision variables	**Base case**	**RON optimized**	**Gross Margin optimized**
Temperature (K)	523	427	447
Adsorption Pressure (bara)	15	13	17
Molar Desorbent / Feed Ratio (%)	30	48	19
Indexing Time (min)	7	7	12

inclusion of iC5 in the Extract. For the SMB cases, a high Recovery (Fig. 5A) is thus inversely proportional to achieving a high RON (Fig. 5B), as only the branched C6 components, 22DMB and 23DMB, have sufficiently high RON to increase the Raffinate RON to 95. In this light, distillation has the fundamental disadvantage that the branched C6 components, owed to their higher boiling point (Table S1), fractionate with the low octane components to the bottoms product (Table S6).

Compared to the performance of conventional distillation summarized in Table S6 and S7, the SMB cases consumed no steam, which substantially reduces the GHG emissions associated with steam generation via natural gas combustion. Compared to 11 MW of steam duty associated with conventional distillation, the SMB unit utilized 3.4 MW and 5.7 MW of electricity when optimizing the RON and the Gross Margin respectively (Table S7). Cooling water duties were markedly lower for the optimized SMB cases at 2.4 MW (RON) and 3.4 MW (Gross Margin) than for distillation at 12.5 MW (Table S7), given the high distillation reflux ratio. The marginal boiling point difference between the linear and branched alkanes necessitated the high reflux ratio of 10 and a distillation tower with 90 stages (Table S5), entailing appreciable operating cost and capital burden. The high relative volatility of the distillation feed also required a high pressure tower (Table S5), further increasing the capital burden. Compared to conventional distillation as measured by Gross Margin, the optimized SMB cases increased the economic return by 47 % when maximizing the RON and by 82 % when maximizing the Gross Margin (Fig. 5C). Therefore, this study motivated for rapid capital investment into retrofitting isomerization facilities with SMB unit operations, replacing outmoded distillation as the primary separation technology.

5. Conclusion

This study aimed to develop a highly efficient adsorption separation technology that can contribute significantly to the sustainability and economics of the overall “well-to-wheel” outcome for LDV fleets globally. This study delivered a fuel with higher Research Octane Number (RON), enabling lower emissions associated with recalibrated LDV engines. After maximizing the RON using a genetic algorithm, a RON of 95 was achievable. Compared to conventional distillation, the SMB cases consumed no steam, which substantially reduces the GHG emissions associated with steam generation via natural gas combustion. Compared to 11 MW of steam duty associated with conventional distillation, SMB

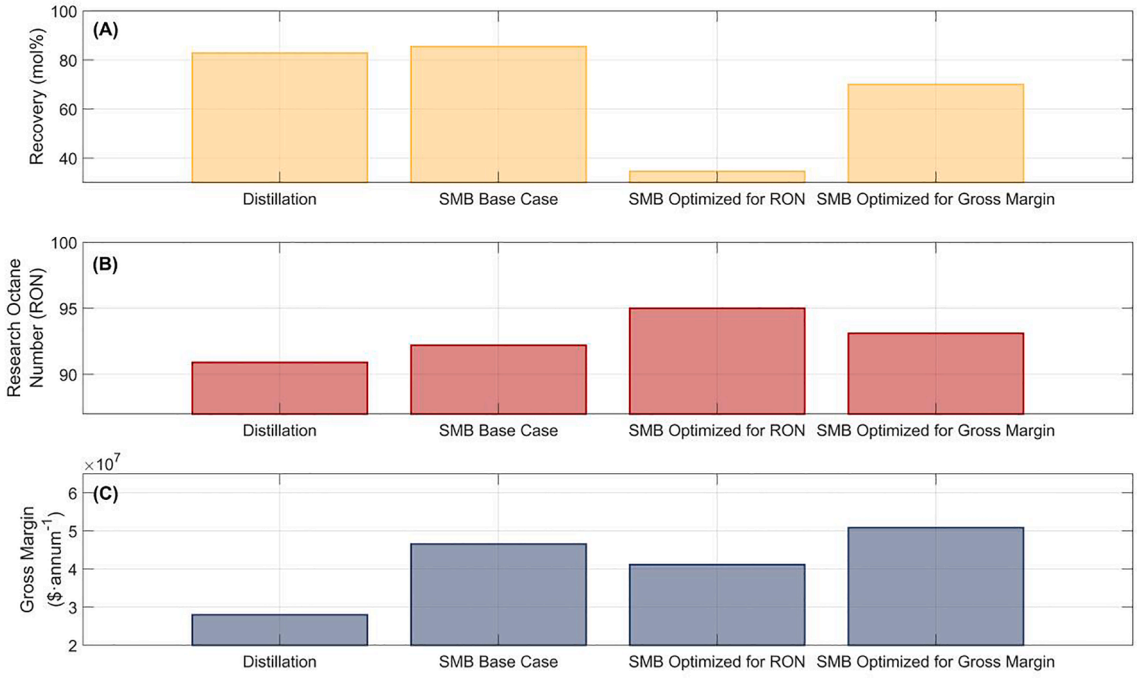

Fig. 5. Comparison of the Recovery (A), the Research Octane Number (B) and the Gross Margin (C) between Distillation, the SMB base case and the optimized SMB cases, i.e. optimized for RON and Gross Margin, as the separation technologies.

utilized 3.4 MW and 5.7 MW of electricity when optimizing the RON and the Gross Margin respectively. Cooling water duties were markedly lower for the optimized SMB cases at 2.4 MW (RON) and 3.4 MW (Gross Margin) than for distillation at 12.5 MW. SMB thus contributes to greater resource resilience and sustainability. Finally, compared to conventional distillation as measured by Gross Margin, the optimized SMB cases increased the economic return by 47 % when maximizing the RON and by 82 % when maximizing the Gross Margin. In summary, this study motivated for rapid capital investment into retrofitting isomerization facilities with SMB unit operations, replacing outmoded distillation as the primary separation technology. Future work will focus on optimizing the separation technology alongside the overall isomerization process using a rigorous techno-economic analysis as objective function for optimisation.

CRediT authorship contribution statement

Tasneem Muhammed: Conceptualization, Data curation, Formal analysis, Investigation, Methodology, Software, Visualization, Writing – original draft, Writing – review & editing. **Begum Tokay:** Conceptualization, Funding acquisition, Project administration, Resources, Supervision, Writing – review & editing. **Alex Conradie:** Conceptualization, Methodology, Visualization, Supervision, Writing – review & editing.

Declaration of Competing Interest

The authors declare that they have no known competing financial interests or personal relationships that could have appeared to influence the work reported in this paper.

Data availability

Data will be made available on request.

Acknowledgments

The authors would like to thank Dr Paul Langston for valuable discussions. This work was supported by the Dean of Engineering Research Scholarship for International Excellence from the University of Nottingham (grant number RFDX42DB2).

Appendix A. Supplementary data

Supplementary data to this article can be found online at https://doi.org/10.1016/j.fuel.2022.126864.

References

[1] Speth RL, Chow EW, Malina R, Barrett SRH, Heywood JB, Green WH. Economic and environmental benefits of higher-octane gasoline. Environ Sci Tech 2014;48 (12):6561–8. https://doi.org/10.1021/es405557p. 0013-936X.
[2] Leone TG, Anderson JE, Davis RS, Iqbal A, Reese II RA, Shelby MH, et al. The effect of compression ratio, fuel octane rating, and ethanol content on spark-ignition engine efficiency. Environ Sci Technol 2015;49(18):10778–89. https://doi.org/10.1021/acs.est.5b01420. 0013-936X.
[3] Sullivan D, Metro S, Pujadó PR. Isomerization in petroleum processing. In: Treese SA, Jones DS, Pujadó PR, editors. Handbook of petroleum processing. Springer International Publishing; 2015. p. 479–97.
[4] Graeme S, Ross J. Advanced solutions for paraffins isomerization. Marriott Rivercenter Hotel San Antonio, TX: National Petrochemical & Refiners Association, National Petrochemical & Refiners Association; 2004. p. 1–26.
[5] Yasakova EA, Sitdikova AV, Achmetov AF. Tendency of isomerization process development in Russia and foreign countries. Oil Gas Bus 2010. 665.656.2, http://www.ogbus.ru/eng/.
[6] Rice LH. Isomerization process. US Patent 7 223 898 B2 2007.
[7] Mohamed MF, Shehata WM, Abdel Halim AA, Gad FK. Improving gasoline quality produced from MIDOR light naphtha isomerization unit. Egypt J Pet 2017;26(1): 111–24. https://doi.org/10.1016/j.ejpe.2016.02.009. 11100621.
[8] p.l. Axens. Isomerization: high octane C5/C6 cuts via isomerization processes. Axens IFP Group Technologies; 2009.
[9] Valavarasu G, Sairam B. Light naphtha isomerization process: a review. Pet Sci Technol 2013;31(6):580–95. https://doi.org/10.1080/10916466.2010.504931. 1091-6466.
[10] Kaiser MJ, de Klerk A, Gary JH, Handwerk GE. Petroleum refining: technology, economics, and markets. 6th edn. CRC Press; 2019.
[11] Silva JAC, Rodrigues AE. Fixed-bed adsorption of n-pentane/isopentane mixtures in pellets of 5A Zeolite. Ind Eng Chem Res 1997;36(9):3769–77. S0888-5885(97) 00158-9.
[12] Silva JAC, Rodrigues AE. Separation of n/iso-paraffins mixtures by pressure swing adsorption. Sep Purif Technol 1998;13:165–208. 1383-5866/98/$19.00 © 1998 PII_S1383-5866_(98)_00043-4.
[13] Silva JAC, Rodrigues AE. Multisite Langmuir model applied to the interpretation of sorption of n-paraffins in 5A zeolite. Ind Eng Chem Res 1999;38(6):2434–8.

[14] Silva JAC, Da Silva FA, Rodrigues AE. Separation of n/iso paraffins by PSA. Sep Purif Technol 2000;20(1):97–110. 1383-5866/00/$.
[15] Bárcia PS, Silva JAC, Rodrigues AE. Separation of branched hexane isomers on zeolite BETA. Adsorpt Sci Technol 2007;25(3/4):169–83.
[16] Bárcia PS, Silva JAC, Rodrigues ArE. Octane upgrading of C5/C6 light naphtha by layered pressure swing adsorption. Energy Fuels 2010;24(9):5116–30. https://doi.org/10.1021/ef100361e. 0887-0624, 1520-5029.
[17] Bárcia PS, Silva JAC, Rodrigues ArE. Adsorption dynamics of C5−C6 isomerate fractions in zeolite Beta for the octane improvement of gasoline. Energy Fuels 2010;24(3):1931–40. https://doi.org/10.1021/ef9013289. 0887-0624, 1520-5029.
[18] Zhang L, Qian G, Liu Z, Cui Q, Wang H, Yao H. Adsorption and separation properties of n-pentane/isopentane on ZIF-8. Sep Purif Technol 2015;156:472–9. https://doi.org/10.1016/j.seppur.2015.10.037. 13835866.
[19] Henrique A, Rodrigues AE, Silva JAC. Separation of hexane isomers in ZIF-8 by fixed bed adsorption. Ind Eng Chem Res 2018;58(1):378–94. https://doi.org/10.1021/acs.iecr.8b05126. 0888-5885, 1520-5045.
[20] Gor GY, Paris O, Prass J, Russo PA, Ribeiro Carrott MM, Neimark AV. Adsorption of n-pentane on mesoporous silica and adsorbent deformation. Langmuir 2013;29 (27):8601–8. https://doi.org/10.1021/la401513n. 1520–5827 (Electronic), 0743–7463 (Linking).
[21] Fu H, Qin H, Wang Y, Liu Y, Yang C, Shan H. Adsorption and separation of n/iso-pentane on zeolites: A GCMC study. J Mol Graph Model 2018;80(59–66). https://doi.org/10.1016/j.jmgm.2017.12.003. 1873 4243 (Electronic), 1093–3263 (Linking).
[22] Abdelrasoul A, Zhang H, Cheng C-H, Doan H. Applications of molecular simulations for separation and adsorption in zeolites. Microporous Mesoporous Mater 2017;242:294–348. https://doi.org/10.1016/j.micromeso.2017.01.038.
[23] Knaebel KS, Hill FB. Pressure swing adsorption: development of an equilibrium theory for gas separations. Chem Eng Sci 1985;40(12):2351–60. https://doi.org/10.1016/0009-2509(85)85139-3.
[24] Leprince P, Travers C. Isomerization of light paraffins. In: Leprince P, Travers C, editors. Petroleum refining: conversion processes. Paris: Editions Technip; 2001. p. 229–56.
[25] Leprince P, Deschamps A, Jullian S. Adsorption in the Oil and Gas Industry, in, Petroleum Refining 2001;Vol. 3:573–91.
[26] Holcombe TC, Sager TC, Volles WK, Zarchy A. Isomerization process. US Patent 4 929 799 1990.
[27] Holcombe TC. Total isomerization process. US Patent 4 210 771 1980; US4210771A.
[28] Stine M. Processes to improve the qualities of distillates: isomerization. In: Encyclopaedia of hydrocarbons: refining and petrochemicals. UOP LLC; 2004. p. 171–80.
[29] Leprince P, Deschamps A, Jullian S. Adsorption. In: Petroleum refining. Paris: Conversion Processes; 2001. p. 525–72.
[30] Evans WE, Stem SC. Isomerization process with recycle of mono-methyl-branched paraffins and normal paraffins. US Patent 4 804 802 1988.
[31] Haensel V. Combination process of isomerization and a sorption process followed by selective fractionation. US Patent 2 966 528 1960.
[32] Stem SC, Evans WE. Total isomerization process with mono-methyl-branched plus normal paraffin recycle stream. US Patent 4 717 784 1987.
[33] Zarchy AS, Amawalk NY, Symoniak MF, Greensboro NC. Isomerization with distillation and PSA recycle streams. US Patent 5 245 102 1993.
[34] Meyers RA. Handbook of petroleum refining processes. 3rd edn. 2004.
[35] Rodrigues A. Simulated moving bed technology: principles, design and process applications. Elsevier Science; 2015.
[36] Pais LS, Loureiro JM, Rodrigues AE. Modeling strategies for enantiomers separation by SMB chromatography. AIChE J 1998;44(3):561–9. https://doi.org/10.1002/aic.690440307.
[37] Broughton DB, Gerhold CG. Continuous sorption process employing fixed bed of sorbent and moving inlets and outlets. US Patent 2 985 589 1961.
[38] Lu ZP, Ching CB. Dynamics of simulated moving-bed adsorption separation processes. Sep Sci Technol 1997;32(12):1993–2010. https://doi.org/10.1080/01496399708000750.
[39] Do DD, Rice RG. Validity of the parabolic profile assumption in adsorption studies. AIChE J 1986;32(1):149–54. https://doi.org/10.1002/aic.690320118. 0001-1541.
[40] Kikkinides ES, Yang RT, Cho SH. Concentration and recovery of carbon dioxide from flue gas by pressure swing adsorption. Ind Eng Chem Res 1993;32(11): 2714–20. https://doi.org/10.1021/ie00023a038.
[41] Chue KT, Kim JN, Yoo YJ, Cho SH, Yang RT. Comparison of activated carbon and Zeolite 13X for CO2 recovery from flue gas by pressure swing adsorption. Ind Eng Chem Res 1995;34(2):591–8. https://doi.org/10.1021/ie00041a020. 0888-5885.
[42] Ruthven DM, Farooq S, Knaebel KS. Pressure swing adsorption. VCH Publishers; 1994.
[43] Vojtesek J, Dostál P, Maslan M. Modelling and simulation of water tank. Comput Sci 2014:pp. https://doi.org/10.7148/2014-0297.
[44] Yang RT. Gas separation by adsorption processes. Elsevier Science; 2013.
[45] Smith GD, Smith GD. Numerical solution of partial differential equations: finite difference methods. Clarendon Press; 1985.
[46] AlRamadan AS, Sarathy SM, Badra J. Unraveling the octane response of gasoline/ethanol blends: paving the way to formulating gasoline surrogates. Fuel 2021;299: 120882. https://doi.org/10.1016/j.fuel.2021.120882. 0016-2361.
[47] Anderson JE, Kramer U, Mueller SA, Wallington TJ. Octane numbers of ethanol– and methanol–gasoline blends estimated from molar concentrations. Energy Fuels 2010;24(12):6576–85. https://doi.org/10.1021/ef101125c.
[48] Rankovic N, Bourhis G, Loos M, Dauphin R. Understanding octane number evolution for enabling alternative low RON refinery streams and octane boosters as transportation fuels. Fuel 2015;150:41–7. https://doi.org/10.1016/j.fuel.2015.02.005.
[49] Chemical Engineering. Chemical engineering's plant cost index. 2022.